

# Transformation texture of allotriomorphic ferrite in steel

D. W. Kim<sup>1</sup>, R. S. Qin<sup>1</sup> and H. K. D. H. Bhadeshia<sup>\*1,2</sup>

Many aspects of the crystallographic texture which develops when austenite transforms into martensite or bainite are well established because the process by which the parent lattice is transformed into that of the product is mathematically defined. This is not the case when the ferrite forms by a reconstructive mechanism. The allotriomorphic ferrite nucleates heterogeneously at austenite grain boundaries, and although a reproducible, low energy orientation relationship is expected to exist between the ferrite and one of the austenite grains with which it is in contact, there are reports that the ferrite can simultaneously adopt this orientation with more than one austenite grain. The authors examine this possibility using crystallographic theory in order to assess the probability of such events as a function of the strength of the texture within the austenite before its transformation.

**Keywords:** Allotriomorphic ferrite, Steel, Texture, Dual orientation

## Introduction

With the advent and popularity of electron backscattered diffraction and orientation imaging microscopy,<sup>1–3</sup> there has been renewed interest in the concept of crystallographic grain size as opposed to the metallographic grain size. The latter is a measure of the amount of grain surface per unit volume, irrespective of the misorientations between adjacent grains as long as the boundaries can be detected by the metallographic method used. The former on the other hand, indicates distances over which there is little variation in crystallographic orientation in spite of intervening grain boundaries. The crystallographic grain size is particularly relevant in understanding the toughness of steels because it determines the percolation and roughness of cracks through the structure.<sup>4–9</sup> Whereas a great deal is known about the control of the metallographic grain size, work on crystallographic grain size control is in its infancy. The mathematical framework needed to perform this would rely on the ability to calculate transformation textures.

In the case of displacive transformations such as bainite and martensite, the set consisting of the orientation relationship, shape deformation and habit plane is uniquely defined by the phenomenological theory of martensite.<sup>10–12</sup> It follows that given the orientation distribution of the austenite grains, that of each martensite plate can be calculated relative to the sample reference frame in order to estimate the crystallographic texture, including the effects of variant selection due to an externally imposed system of stresses.<sup>13–16</sup> An interesting simplification is that because

martensite plates are confined to the grains in which they grow, it is not necessary to identify the relative physical locations of individual austenite grains in order to calculate the texture; the calculations can be conducted independently for each austenite grain and then summed to give the overall texture.

The situation is rather different for transformations which involve the diffusion of all atoms (allotriomorphic ferrite, pearlite), because the transformation products are then able to traverse austenite grain boundaries,<sup>17–19</sup> as illustrated in Fig. 1*a*. The conventional wisdom is that an allotriomorphic  $\alpha$  will nucleate at an austenite grain boundary with a low energy orientation relationship with one of the austenite  $\alpha/\gamma_2$  grains and a random orientation with the other grain  $\alpha/\gamma_1$  with which it has contact. One side of the allotriomorph will then have a faceted appearance and the other should exhibit a curved boundary.

There is, however, longstanding evidence to suggest that an allotriomorph may have a low energy orientation with both the adjacent austenite grains.<sup>20–23</sup> These conclusions naturally depend on the degree of deviation from the low energy orientation. The purpose of the present work was to examine theoretically the chances of an allotriomorph simultaneously achieving a low energy orientation with both the adjacent austenite grains, as a function of the texture of the original austenite and the precision with which a low energy orientation is defined. Unlike martensite, it is necessary in such a model to define the neighbours and orientations of each austenite grain.

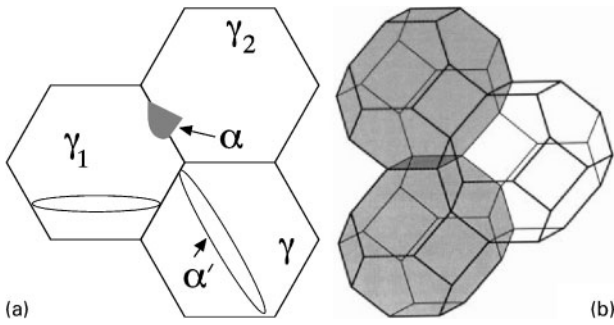
## Austenite grain structure

Austenite grains are conveniently represented as a stack of identical, space filling Kelvin tetrakaidecahedra,<sup>24–28</sup> each of which consists of eight hexagonal and six square faces, with 36 equal edges, as illustrated in Fig. 1*b*. For ferrite nucleation at austenite grain surfaces, there are therefore 14 face sites per grain.

<sup>1</sup>Graduate Institute of Ferrous Technology (GIFT), Pohang University of Science and Technology (POSTECH), Pohang 790 784, Korea

<sup>2</sup>Department of Materials Science and Metallurgy, University of Cambridge, Pembroke Street, Cambridge, CB2 3QZ, UK

\*Corresponding author, email hkdb@cam.ac.uk



1 a martensite plates are confined to austenite grain in which they nucleate whereas allotriomorphs are not ( $\alpha$  and  $\gamma_2$  are in low energy orientation whereas that between  $\alpha$  and  $\gamma_1$  will in general be random) and b space filling stack of tetrakaidecahedra with a few of neighbours defined

The computer algorithm was constructed so that for each grain orientation relative to the sample frame of reference, it was possible to access the orientations of the 14 neighbouring grains. A total of 1700 austenite grains were created in this way, with one of the grains having its crystallographic axes exactly parallel to those of the sample.

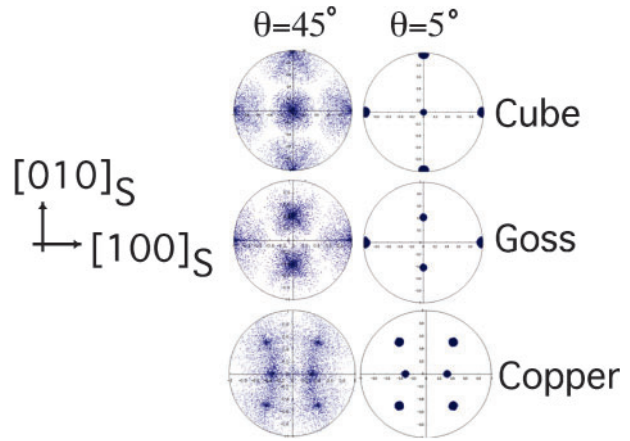
The relationship between the sample and austenite crystal axes can be described using Euler angles  $\phi_1$ ,  $\phi$  and  $\phi_2$ . These are the three angles by which the sample reference frame must be rotated in order to coincide with that of the crystal. The rotation matrix relating the frames is given by

$$\begin{pmatrix} \cos\phi_1\cos\phi_2 - \sin\phi_1\cos\phi\sin\phi_2 \\ -\cos\phi_1\sin\phi_2 - \sin\phi_1\cos\phi\cos\phi_2 \\ \sin\phi_1\sin\phi \\ \sin\phi_1\cos\phi_2 + \cos\phi_1\cos\phi\sin\phi_2 \\ -\sin\phi_1\sin\phi_2 + \cos\phi_1\cos\phi\cos\phi_2 \\ -\cos\phi_1\sin\phi \\ \sin\phi\sin\phi_2 \\ \sin\phi\cos\phi_2 \\ \cos\phi \end{pmatrix} \quad (1)$$

To generate a random set of austenite grain orientations, the Euler angles  $\phi_1$  and  $\phi_2$  (ranging from 0 to  $2\pi$ ) and the value of  $\cos\phi$  (between  $\pm 1$ ) were selected using a random number generator.<sup>15,29</sup> Non-random austenite textures were generated relative to the sample axes by setting the first austenite grain to the exact required texture, and then choosing relative to this grain, random rotation axes but with the right handed rotation angle limited to the range  $\theta=0$  to  $45^\circ$ ;<sup>13</sup> the Goss, cube and copper textures were generated in this way and the effect of the limiting value of  $\theta$  is illustrated in Fig. 2.

### Introduction of ferrite

Any grain of ferrite will always have an orientation relationship ( $\alpha \mathbf{J} \gamma$ ) with an austenite grain. (Throughout the present paper, the authors use the vector and matrix notation due to Bowles and MacKenzie which is particularly good at avoiding confusion between frames



2 Modelled austenite textures as function of limiting value of  $\theta$ :  $\langle 100 \rangle_\gamma$  pole figures are all plotted relative to sample axes 'S'

Refs. 10, 30 and 31.) However, some ferrite grains will have a special orientation relationship which corresponds to a low energy configuration; this is often assumed to be that due to Kurdjumov–Sachs<sup>32</sup> or Nishiyama–Wassermann.<sup>33,34</sup> However, the most coherent relationships even in reconstructive transformations are likely to be irrational because for usual lattice parameter ratios, the Kurdjumov–Sachs and Nishiyama–Wasserman orientations do not lead to an invariant line between  $\alpha$  and  $\gamma$ .<sup>35</sup> The authors therefore adopt as the low energy orientation, one predicted by the crystallographic theory of martensite in order to ensure a coherent line between  $\alpha$  and  $\gamma$ :<sup>31</sup>

$$(\gamma \mathbf{J}_{LE} \alpha) = \begin{pmatrix} 0.579356 & 0.542586 & 0.102537 \\ 0.014470 & 0.133650 & -0.788984 \\ -0.552000 & 0.572979 & 0.086936 \end{pmatrix} \quad (2)$$

Here the subscript in  $\mathbf{J}_{LE}$  implies that this coordinate transformation represents a low energy orientation. Thus

$$\begin{aligned} (1 \bar{1} 1)_\gamma &= (0.012886 \ 0.981915 \ 0.978457)_\alpha \\ [0 \ 1 \ 1]_\gamma &= [\bar{0}.53753 \ 0.706629 \ \bar{0}.702048]_\alpha \end{aligned}$$

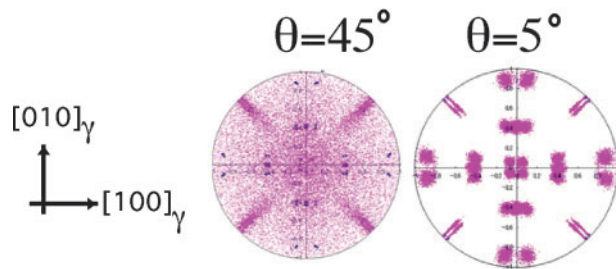
This means that  $(1 \bar{1} 1)_\gamma$  is  $0.54^\circ$  from  $(0 \ 1 \ 1)_\alpha$  and very nearly parallel though not exactly parallel to  $(0 \ 1 \ 1)_\alpha$  and  $[0 \ 1 \ 1]_\gamma$  is  $6.91^\circ$  from  $[\bar{1} \ 1 \ \bar{1}]_\alpha$ . This is close to the Kurdjumov–Sachs orientation but is irrational and allows for the existence of a coherent line between the two lattices.

When ferrite was allowed to form on a face between two austenite grains with relative orientation  $(\gamma_1 \mathbf{J} \gamma_2)$  (Fig. 1a), the corresponding orientations with the ferrite are  $(\gamma_1 \mathbf{J} \alpha)$  and  $(\gamma_2 \mathbf{J}_{LE} \alpha)$  where the latter is the low energy variant. It follows that

$$(\gamma_1 \mathbf{J} \alpha) = (\gamma_1 \mathbf{J} \gamma_2)(\gamma_2 \mathbf{J}_{LE} \alpha) \quad (3)$$

Both the matrices on the right hand side of this equation are known because the austenite orientations are set initially and  $(\gamma_2 \mathbf{J}_{LE} \alpha)$  is given by equation (2).

Ferrite was allowed to nucleate on all 14 faces of each austenite grain. The ferrite in all cases had a low energy orientation with one austenite grain; since there are 24



**3**  $\langle 100 \rangle_\alpha$  pole figures showing calculated ferrite textures, plotted relative to austenite frame of reference, as function of strength of texture as defined by angle  $\theta$

crystallographically equivalent such orientations for any given austenite grain, the selection of the particular variant was made at random from the 24 available.

The possibility that  $(\gamma_1 \mathbf{J} \alpha)$  is close to a low energy orientation was investigated by studying its deviation from all 24 variants of  $(\gamma_1 \mathbf{J}_{LE} \alpha)$ . This is performed by calculating

$$(\gamma_1 \Delta \mathbf{J} \gamma_1) = (\gamma_1 \mathbf{J} \alpha)(\alpha \mathbf{J}_{LE} \gamma_1) \quad (4)$$

where  $(\alpha \mathbf{J}_{LE} \gamma_1)$  is the inverse of  $(\gamma_1 \mathbf{J}_{LE} \alpha)$ . The axis angle pair corresponding to  $\Delta \mathbf{J}$  was calculated; because of the symmetry of the cubic system, for each axis angle pair there are 23 crystallographically equivalent sets. The particular set with the lowest angle of rotation  $\Delta$  was selected to assess the closeness of the orientation  $(\gamma_1 \mathbf{J} \alpha)$  to the low energy case. The case where a ferrite grain has an exact low energy orientation with one austenite grain, and at the same time an approximately low energy orientation (as defined by the maximum permitted deviation  $\Delta = \Delta_{max}$ ) with the adjacent austenite grain is henceforth referred to as a dual orientation for convenience.

The procedure was repeated for every single ferrite grain and the resulting transformation texture studied alongside the probability of finding a dual orientation.

## Calculated ferrite textures

It is important to note that the issue is to find the probability of the dual orientation phenomenon. The ferrite orientations are therefore studied relative to those of the austenite grains. In contrast, the texture of the austenite before transformation is defined relative to the sample frame of reference. The orientation of the austenite texture relative to the sample axes is not relevant to the prediction of the transformation texture relative to the austenite frame of reference. For this

**Table 1** Calculated percentages of dual orientation as function of strength of austenite texture (related to angle  $\theta$ ): dual orientation is here defined for all orientations within  $\Delta_{max}=15^\circ$  of low energy orientation

$\theta$	% dual orientation			
	Random	Cube	Goss	Copper
5		37.6	37.9	37.2
15		31.3	30.2	30.6
25	0.8	17.9	20.9	20.5
35		12.2	12.2	12.2
45		8.5	7.6	9.2

reason, the results presented in Fig. 3 and Tables 1 and 2 are almost identical for all three varieties of austenite texture (Goss, cube and copper), any differences arising because of the stochastic process of generating the initial austenite textures.

It is worth pointing out that in Table 1, the percentage of dual orientation is exceptionally large when  $\Delta_{max} \geq \theta$ . This is expected since the misorientations between austenite grains are then smaller than the spread allowed in the definition of the state of dual orientation.

The results are interesting because the chance of obtaining a dual orientation when the austenite grains are randomly disposed is found to be negligible. The probability naturally increases as the polycrystalline aggregate tends towards a stronger texture (lower  $\theta$ ), i.e. towards a single crystal.

It should be emphasised that a value of  $\Delta_{max}$  as large as  $15^\circ$  is a substantial deviation from the low energy orientation and in general cannot be capable of sustaining an invariant line between the  $\gamma$  and  $\alpha$ . The same applies to  $\Delta_{max}=5^\circ$  so the concept of dual orientation should not be taken to imply that both sides of the allotriomorph (i.e.  $\alpha/\gamma_1$  and  $\alpha/\gamma_2$ ) are capable of developing into displacive transformation products such as Widmansättten ferrite<sup>36,37</sup> as is sometimes implied.<sup>17,38</sup> Displacive transformation requires the existence of the invariant line.<sup>39</sup> This means that any observation of Widmansättten ferrite developing from the deviant  $\alpha/\gamma_1$  side of the allotriomorph will have a low misorientation boundary between the Widmansättten ferrite and allotriomorphic ferrite. Such misorientations should be detectable using electron backscattered diffraction methods.

In order to decide on the significance of a particular kind of dual orientation associated with a specific value of  $\Delta_{max}$ , it is necessary to define a purpose for calculating or measuring the probability of dual orientations. For example, when considering the percolation of cracks through the polycrystalline aggregate, it is the parallelism of cleavage planes in different grains along the crack path that matters. The angle through which the cleavage plane must deviate in order to arrest or significantly retard its propagation can be used to decide on an appropriate value of  $\Delta_{max}$ .

## Grain edge and corner nucleation

When ferrite nucleates at austenite grain edges it is in contact with three austenite grains. Since the assumption is that the ferrite has a low energy orientation with one of these austenite grains, the chance of obtaining a dual

**Table 2** Calculated percentages of dual orientation as function of strength of austenite texture (related to angle  $\theta$ ): dual orientation is here defined for all orientations within  $\Delta_{max}=5^\circ$  of low energy orientation

$\theta$	% dual orientation			
	Random	Cube	Goss	Copper
5		6.3	7.1	6.6
15		2.8	2.8	2.7
25	0	1.27	1.54	1.42
35		0.73	0.83	0.75
45		0.50	0.67	0.50

orientation with at least one of the remaining two austenite grain doubles. Thus in Table 1 all of the percentages can be doubled to represent edge nucleation.

In the case of corner nucleation, the ferrite grain is in contact with four austenite grains so that the possibility of dual orientation triples. This means that when  $\Delta_{\max} \geq \theta$ , the chance becomes 100%, although as emphasised previously, the relevance of a dual orientation diminishes as  $\Delta_{\max}$  increases relative to the strength of the austenite texture.

Although the activation energy for heterogeneous nucleation decreases in the order face→edge→corner, the number density of nucleation sites also decreases in the same order. For this reason, corner nucleation dominates at low undercoolings below the equilibrium transformation temperature and grain face nucleation at large undercoolings.<sup>40</sup> It follows that the chances of obtaining dual orientations are larger when transformations are carried out at low undercoolings or at very slow cooling rates during continuous cooling.

## Summary

If the concept of *dual orientation* is taken to imply that exact variants of a strict low energy orientation relationship exists between an allotriomorph and more than one adjacent austenite grain, then the probability of this happening is negligibly small even in strongly textured austenite.

However, if the definition is less exacting with deviations of 5° or more permitted, then there is a detectable chance of finding such allotriomorphs. Care must be exercised in setting the level of deviation by identifying the purpose of the work so that the interpretation of the outcome can be treated in context.

The calculations here do not allow for experimental error in the determination of orientation relationships, which must add to the chances of falsely detecting dual orientations.

It is suggested therefore that any experimental study of the dual orientation phenomenon should report the parameters  $\Delta_{\max}$ ,  $\theta$  and the error of the experimental method used.

The computer programs developed for the present work are available freely on [www.msm.cam.ac.uk/map/mapmain.html](http://www.msm.cam.ac.uk/map/mapmain.html)

## Acknowledgements

The authors are grateful to Professor Hae-Geon Lee for the provision of laboratory facilities at GIFT. The authors also appreciate helpful discussions with Dr S. Kundu of TATA Steel.

## References

1. D. J. Dingley and M. M. Nowell: *Microchim. Acta*, 2004, **147**, 157–165.

2. F. J. Humphreys: *Scr. Mater.*, 2004, **51**, 771–776.
3. A. F. Gourgues-Lorenzon: *Int. Mater. Rev.*, 2007, **52**, 65–128.
4. A. F. Gourgues, H. M. Flower and T. C. Lindley: *Mater. Sci. Technol.*, 2000, **16**, 26–40.
5. A.-F. Gourgues: *Mater. Sci. Technol.*, 2002, **18**, 119–133.
6. J. Nohava, P. Hausild, M. Karlik and P. Bompard: *Mater. Charact.*, 2003, **49**, 211–217.
7. A. Lambert-Perlade, A. F. Gourgues, J. Besson, T. Sturel and A. Pineau: *Metall. Mater. Trans. A*, 2004, **35A**, 1039–1053.
8. Y. M. Kim, S. Y. Shin, H. Lee, B. Hwang, S. Lee and N. J. Kim: *Metall. Mater. Trans. A*, 2007, **38A**, 1731–1742.
9. V. Callone, A. F. Gourgues and A. Pineau: *Fatig. Fract. Eng. Mater. Struct.*, 2004, **27**, 31–43.
10. J. S. Bowles and J. K. MacKenzie: *Acta Metall.*, 1954, **2**, 129–137.
11. J. K. MacKenzie and J. S. Bowles: *Acta Metall.*, 1954, **2**, 138–147.
12. M. S. Wechsler, D. S. Lieberman and T. A. Read: *Trans. AIME J. Met.*, 1953, **197**, 1503–1515.
13. S. Kundu and H. K. D. H. Bhadeshia: *Scr. Mater.*, 2006, **55**, 779–781.
14. S. Kundu: 'Transformation strain and crystallographic texture in steels', PhD thesis, University of Cambridge, Cambridge, UK, 2007.
15. S. Kundu, K. Hase and H. K. D. H. Bhadeshia: *Proc. Roy. Soc. A*, 2007, **463A**, 2309–2328.
16. S. Kundu and H. K. D. H. Bhadeshia: *Scr. Mater.*, 2007, **57**, 869–872.
17. H. I. Aaronson: in 'Decomposition of austenite by diffusional processes', (ed. V. F. Zackay and H. I. Aaronson), 387–548; 1962, New York, Interscience.
18. H. K. D. H. Bhadeshia: *Prog. Mater. Sci.*, 1985, **29**, 321–386.
19. R. C. Reed and H. K. D. H. Bhadeshia: *Mater. Sci. Technol.*, 1992, **8**, 421–435.
20. A. D. King and T. Bell: *Metall. Trans. A*, 1975, **6A**, 1419–1429.
21. A. D. King and T. Bell: *Metallography*, 1976, **9**, 397–413.
22. S. S. Babu and H. K. D. H. Bhadeshia: *Mater. Sci. Eng. A*, 1991, **A142**, 209–220.
23. D.-W. Suh, J.-H. Kang, K. H. Oh and H.-C. Lee: *Scr. Mater.*, 2002, **46**, 375–378.
24. E. E. Underwood: 'Quantitative stereology'; 1970, Reading, MA, Addison-Wesley Publication Company.
25. I. Czinege and T. Reti: Proc. 18th Int. Conf. on 'Machine tool design and research', Vol. 1, 159–163; 1977, MacMillan, London.
26. Y. van Leeuwen, S. Vooijs, J. Sietsma and S. V. der Zwaag: *Metall. Mater. Trans. A*, 1998, **29A**, 2925–2931.
27. S. B. Singh and H. K. D. H. Bhadeshia: *Mater. Sci. Technol.*, 1998, **15**, 832–834.
28. Q. Zhu, C. M. Sellars and H. K. D. H. Bhadeshia: *Mater. Sci. Technol.*, 2007, **23**, 757–766.
29. B. J. Bunge: 'Mathematische Methoden der Texturanalyse'; 1982, London, Butterworth.
30. J. W. Christian: 'Theory of transformations in metal and alloys'; 1975, Oxford, Pergamon Press.
31. H. K. D. H. Bhadeshia: 'Geometry of crystals', 2nd edn; 2001, London, Institute of Materials.
32. G. V. Kurdjumov and G. Sachs: *Z. Phys. A*, 1930, **64A**, 325–343.
33. Z. Nishiyama: *Sci. Reports Tohoku Imper. Univ.*, 1934, **23**, 637–634.
34. G. Wassermann: *Arch. Eisenhüttenwes.*, 1933, **6**, 347–351.
35. K. M. Knowles, D. A. Smith and W. A. T. Clark: *Scr. Metall.*, 1982, **16**, 413–416.
36. J. D. Watson and P. G. McDougall: *Acta Metall.*, 1973, **21**, 961–973.
37. H. K. D. H. Bhadeshia: *Mater. Sci. Technol.*, 1985, **1**, 497–504.
38. M. Hillert: in 'Decomposition of austenite by diffusional processes', (ed. V. F. Zackay and H. I. Aaronson), 197–237; 1962, New York, Wiley.
39. J. W. Christian and A. G. Crocker: in 'Dislocations in solids', 165; 1980, Amsterdam, Elsevier.
40. J. W. Cahn: *Acta Metall.*, 1952, **4**, 449–459.